INTERNATIONAL DESIGN CONFERENCE - DESIGN '98
Dubrovnik, May 19 - 22, 1998.

Calculation of Involute Splines under Elastic Material Behaviour

U. Burgtorf, P. Dietz and M. Garzke

Involute Splines, Calculation of Load Capacity, Shaft-Hub-Connection

Abstract: The design of splined joints used in industrial applications frequently results in maximum flank pressure. This often leads to overdimensioning and in certain cases to failure of the shaft-hub connection. The existing german standard DIN 5466 for the calculation of load capacity, when coupled with increasing power densities and weight savings, is an unsatisfactory basis for dimensioning. The principles behind the calculations for the new draft standard, developed by the Institut für Maschinenwesen TU Clausthal, are presented here as well as the main geometric parameters which have an influence: the number of teeth and the width of the splined joint.

1. Introduction

Involute splines with profiles according to the german standard DIN 5480 [DIN 1991] are frequently used for the transfer of torque with simultaneous axial freedom of movement of both shaft and hub. The large number of form elements (tooth pairs) which are engaged allow the transfer of high torques at small outside diameters of hub. Economical applications are opening up particularly in large volume production using metal-cutting and non-chip forming manufacturing processes.
Previous - in part grossly simplified - calculation processes for the tooth design of splined joints, such as the calculation based on maximum permissible flank pressure [Decker 1990] or based on other simple mechanical approximations and test models [Kohl 1986] lead to the overdimensioning of splined joints on account of their numerous simplifications. The complex problematic nature of shaft and hub fits and their resulting influence on the load distribution and load capacity as well as the varying operating conditions lead repeatedly to wear or fracture damage of the form-fitting shaft-hub-connection.
In line with increased performance and safety demands an improved calculation approach is required for the safe design of splined joints. The investigation of operating and loading characteristics on involute splines is the major research topic at the Institut für Maschinenwesen of the TU Clausthal. From the results of extensive numerical and experimental research supported by Forschungsvereinigung Antriebstechnik, Deutsche Forschungsgemeinschaft and Volkswagen-Stiftung a new approach for the calculation of spline geometry has been developed [Wesolowski 1996]. This calculation approach forms the basis for the revision of standard DIN 5466.

2. Damage to involute splines

Durability and load capacity of involute splines are influenced by two entirely different processes: wear and fatigue. Form closure is being "used up" due to wear of the tooth profiles, which leads to an increase in play and eccentricity. The notches in the geometry give rise to stress concentrations, which under static loading result in brittle fracture and under dynamic loading lead to fatigue failure of the joint. The following conclusions are drawn from analysis of the factors which influence joint failure:

· The crack propagation caused by brittle and fatigue fractures mostly starts at a notch in the tooth base on or at a point directly near the ends of the splined joint [Dietz 1978], Fig. 1.

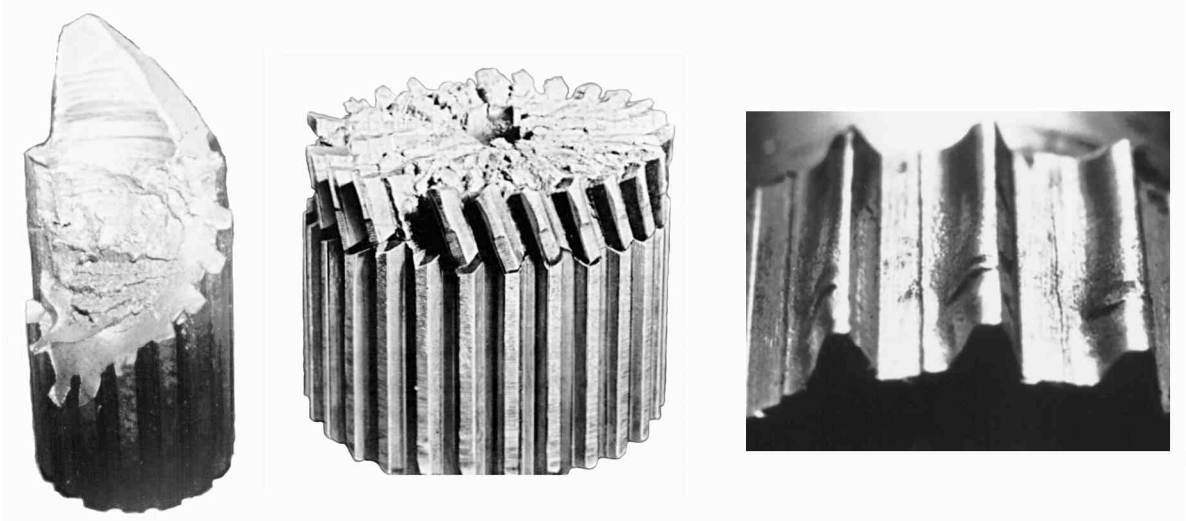

Figure 1. Damage to involute splines. left: fatigue fracture of a spline, middle: brittle fracture, right: appearance of wear

· The deformation behaviour of shaft and hub, and in particular the stiffness jump at the the ends of the splined joint cause an uneven stress distribution over the length of the joint with an excessive load peak at the start of the splined joint [Villmer 1984]. Further load peaks develop through the notch effect resulting from the spline geometry at the tooth base on the shaft and on the hub. The superposition of these load peaks at the point of load introduction creates a complicated triaxial stress state which can promote fatigue fracture [Kohl 1986].
· The load distribution on the individual tooth pairs in a splined joint greatly depends on the play in the teeth and on the quality of the teeth. The cumulative pitch error is therefore a substantial factor in determining the number and the loading of load-bearing tooth pairs as well as the deformation behaviour of the joint [Dietz 1978].
· The load composition of torque and lateral force has a decisive influence on the load distribution on the circumference of the joint and on the relative movement between shaft and hub [Dietz 1978] as well as on the wear behaviour of the joint [Zapf 1986, Schäfer 1995], Fig. 1.
· Involute splines with relative motions represent a tribological system which includes all the significant wear mechanisms - adhesion, abrasion, surface fatigue and tribo-oxidation. Aside from surface reactions in the area of contact, the removal of wear products has a decisive role.

3. Involute splines - loading behaviour

3.1 Load behaviour of involute splines under pure torque

In order to clarify the loading and deformation behaviour of involute splines under torque extensive three-dimensional finite element contact calculations have been carried out. The results of these investigations have lead to a revision of the calculation rules pertaining to DIN 5466. In the example of the torsional loading case the two most significant geometric parameters having an influence on the loading state are considered to be the number of teeth and the width of the splined joint.
The loads in the notch area of the spline under torque result from the force normal to the flank F, which can be resolved into a tangential force, F_U and a radial force F_R. The tangential component produces shear stress in the spline root as well as a tensile load on the loaded side of the tooth (side in tension, subscript z) and a compressive load on the unloaded side (side under compression, subscript d), both due to tooth bending. The radial component causes compressive and tangential stresses. The force normal to the flank on the hub can be split up in exactly the same manner into a circumferential force, F_U and a radial force, F_R. The circumferential component causes shear stress in the tooth root as well as a tensile load on the loaded side. When considering a hub the difference between the loaded

and unloaded side as exists in the shaft can be ignored. Due to the hub width the loading on the tensile side is more critical than on the compressive side of the hub [DIN 1996].
The determination of the contact calculations is carried out through the application of equivalent stress using the von Mises strain energy hypothesis in the area of the spline root on both the compressive side of the shaft as well as the tensile sides of both shaft and hub. Through the comparison of stress distribution in the root of the spline the fundamental differences can be established between joints having small and large numbers of teeth. As an example two splined shafts are shown in Fig. 2 with small (z=6) and large (z=62) numbers of teeth.

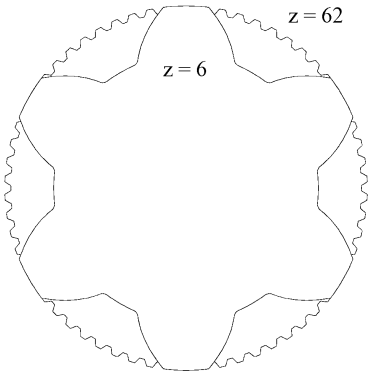

Figure 2. Comparison of the cross section of splined shafts of the same reference diameter with small and large numbers of teeth

The equivalent stress distribution over the length of the spline for both the side in tension and the side under compression of the shaft is plotted in Fig. 3 for both of these splines along with a further joint having z=20 teeth. The joint with z=6 teeth shows no marked peak stress at the start of the joint (a). The maximum equivalent stress occurs in the area before the contact zone, where the influence of tooth bending has died out and a condition of undisturbed torsion exists (u) [Wesolowski 1996]. As the number of teeth increase a marked maximum stress can be recognised at the start of the joint. Due to this, the maximum stress occurs on the side under tension just before the start of the joint and on the side in compression directly at the first contact point of the joint. The cause for this behaviour can be seen in the force transmission path, which runs from the hub to the shaft via the contact zone.
Splined shafts with a smaller number of teeth show higher loading in the area of undisturbed torsion (u) than a joint with more teeth under the same torque load. The reason for this is rooted in the different polar second moments of area of the splined shafts resulting from their differing cross sections, as can clearly seen in the comparison of splined joints with differing numbers of teeth, Fig. 2.

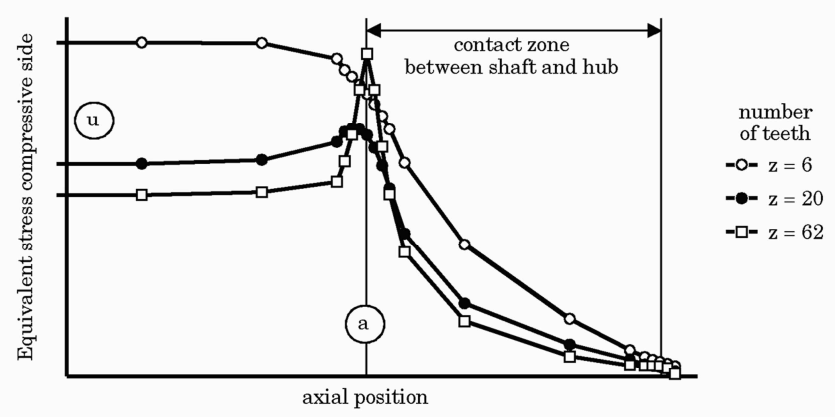

Figure 3. Comparison of the distribution of stress at the spline root over the splined joint width for different numbers of teeth

The inverse proportional relationship between transverse stress and the polar second moment of area ($\tau = T/W_t$) for loading in cylindrical bars under torsion also applies analogously to the calculation of the stresses in the toothed joint. This explains the higher equivalent stresses in a joint with a lower se-

cond moment of area. Splined shafts with a smaller number of teeth are primarily loaded under torsion, splined shafts with a larger number of teeth are subject to specific raised bending loads at the start of the joint.
Through various investigations it has been shown that the maximum stress at the tooth root can only be negligibly reduced by the use of widths of splined joint greater than $b = 0.5 \cdot d_B$ [Wesolowski 1996, Villmer 1984, Schöpf 1976]. With regard to loading of the shaft tooth root, the optimal ratio of width of splined joint to reference diameter is $b/d_B = 0.6$. At the start of the joint, where it behaves like a thin toothed disk the composition of the equivalent stress in the tooth root due to the torsional load component is dependant on the flank load across the width of the splined joint. The equivalent stress in the root of the tooth in the shaft is shown in Fig. 4 for a joint with a medium number of splines and joint widths of $b/d_B = 0.05$ and 0.5. The stresses in a very short joint corresponding to a toothed disk are much higher than in a splined joint of optimal width. In very short splined joints the flank pressure has an almost equal distribution over the width of the joint.

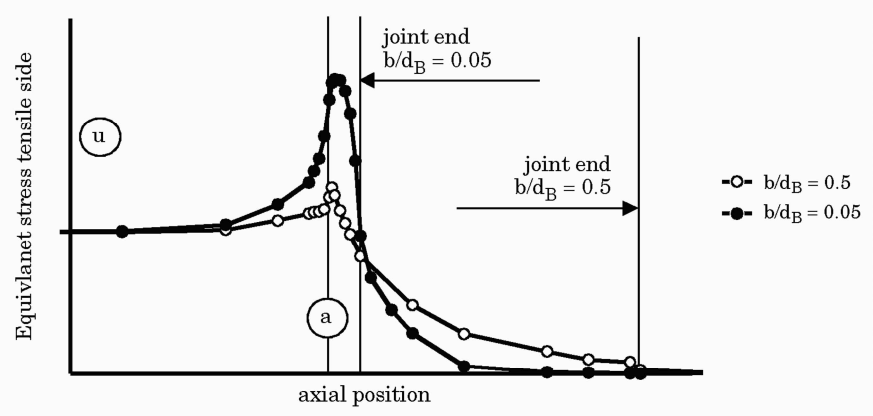

Figure 4. Comparison of stress distribution over the splined joint width in the shaft tooth root for various ratios of width to diameter b/d_B

When using a joint of optimal width a pronounced pressure peak occurs at the start of the joint which falls away towards the end of the joint. The torsional component clearly dominates the maximum equivalent stress in wide joints, whilst in shorter joints and for medium to large numbers of teeth it is the toothed disk or 'tooth bending' behaviour which dominates. However for small numbers of teeth it is torsional loading which fundamentally dominates.

3.2 Determination of resultant load

The maximum flank pressure p_{max} in the disc model of the splined joint, p_s can be calculated for a joint of width b using the maximum force F_{max} normal to the flank. Using this value and through the consideration of a geometry dependant width factor k_b it is possible to calculate the maximum flank pressure in a splined joint. The maximum pressure on the disc model of the joint is required in order to calculate the stresses $\sigma_{s1,z/d}$ (Subscripts: z = loaded side; d = unloaded side) in the area of the notch in the splined shaft, which are due to the flank force F. The calculation approach for the tangential component F_U is equivalent to that of a cantilever spring beam, whilst the radial force F_R equates to that of a solid or hollow shaft subjected to an external pressure. For all other individual loads the maximum loadings in the splined shaft are calculated through the corresponding second moments of area (torsion, bending moment) or cross-sectional areas (lateral and axial force).

	maximum stress in the disc model of the shaft	$\sigma_{s1,z/d}$
	maximum torsional stress	τ_{tmax1}
	maximum bending stress	$\sigma_{bmax1,(a/u)}$
	maximum shear stress due to lateral force	τ_{sn1}
	maximum flank stress (tensile or compressive)	$\sigma_{ax1,(a/u)}$.
Subscripts	1 = shaft; a = start of joint; u = undisturbed area	
	z = loaded side; d = unloaded side	

From the individual stress components the resultant equivalent stress in the notch area of the shaft (fillet at the tooth root) can be calculated. In doing so it is necessary to differentiate between the different areas in which the possible maximum tooth base stress can occur (i.e. in the undisturbed area or in the start of the joint) as well as between the loaded and unloaded sides of the shaft. The resultant equivalent stress at the start of the joint (a) is calculated using Eqn.(1) for the loaded side and using Eqn.(2) for the unloaded side.

$$\sigma_{v1,z,a} = \sqrt{\left(\sigma_{b\max1,a} + k_{ax1,z}\ \sigma_{ax1,a}\right)^2 + \left(k_{s1,z}\ \sigma_{s1,z}\right)^2 + 3\left[\left(k_{t1,z}\ \tau_{t\max1}\right)^2 + \tau_{sn1}{}^2\right]} \qquad (1)$$

$$\sigma_{v1,d,a} = \sqrt{\left(\sigma_{b\max1,a} + k_{ax1,d}\ \sigma_{ax1,a}\right)^2 + \left(k_{s1,d}\ \sigma_{s1,d}\right)^2 + 3\left[\left(k_{t1,d}\ \tau_{t\max1}\right)^2 + \tau_{sn1}{}^2\right]} \qquad (2)$$

Through the use of three correction factors the introduction of flank load directly in the notch area can be taken into consideration. The correction factor k_{ax1} describes the influence the axial force has on the loading combination, factor k_{s1} describes the influence of tooth bending, shear and pressure and factor k_{t1} describes the influence of the torsional force. Due to the stiffness jump experienced in moving from the shaft to the hub the flank pressure reaches its maximum value p_{max} at the joint end on the side of the shaft restraint. This peak occurs only in an extremely localised area. The flank areas outside of the joint in the area immediately next to the highest pressure value experience no external loads. The effects on the stresses in the notch area due to the maximum pressure are diminished through these supported flank areas and are taken into consideration in the calculations through correction factors. In each equation the maximum values of the individual loads are applied for the side under compression and the side in tension.
The influence of the stress component due to tooth bending, shear and pressure completely drops off at a sufficient distance from the start of the joint and the corresponding correction factors tend to zero and can be ignored. The correction factors for torsion and axial force tend to one, because the torsional loading in the notch area is unaffected by the change in stiffness and is distributed uniformly over the cross section of the shaft. The calculation for the equivalent stress in the undisturbed area (u) can therefore be considerably simplified to give Eqn.(3).

$$\sigma_{v1,u} = \sqrt{\left(\sigma_{b\max1,u} + \sigma_{ax1,u}\right)^2 + 3\left[\tau_{t\max1}{}^2 + \tau_{sn1}{}^2\right]} \qquad (3)$$

In order to ascertain the critical stress in the notch area of the shaft the individual resultant equivalent stresses from Eqn.(1) to Eqn.(3) are compared with one another and the maximum stress value taken. The equivalent stress is separately calculated for static and dynamic load cases.
The calculation of the loading in the toothed hub follows analogously the calculation for the toothed shaft. The centrifugal force at high hub rotation speeds adds a further stress component and the smaller shear stress contribution of the lateral force in hubs is neglected:

maximum stress in the disc model of the hub	σ_{s2}
maximum torsional stress	σ_{tmax2}
maximum bending stress	σ_{bmax2}
maximum flank stress (tensile or compressive)	σ_{ax2}
maximum centrifugal stress	$\sigma_{\omega max2}$

Subscripts : 2 = hub

From the individual loading components the resultant equivalent stress can be calculated in the notch area of the hub (fillet radius at tooth root). The calculation differentiates first of all between joints with shaft protrusion on both sides and those with hub protrusion on only one side. This is necessary because in the case of protrusion at the joint end (e) bending stress can arise, which can't be neglected. In

thin walled shafts the equivalent stress is determined at both joint ends (Subscript a: start of joint, side of shaft clamping; subscript e: joint end), in thick walled hubs calculation at the start of the joint (a) is sufficient.
In contrast to the calculation of the notch loads in the disc model of the shaft it is sufficient when considering a hub to determine the resultant loading on the side in tension, since this side is more critical due to the hub expansion than the side under compression. The resultant equivalent stress is calculated at the joint start (a) using Eqn.(4) and for thin walled hubs is additionally calculated at the end of the joint (e) using Eqn.(5).

$$\sigma_{v2,a} = \sqrt{\left(k_{ax2,a} \ \sigma_{ax2} \right)^2 + \left(k_{s2,a} \ \sigma_{s2} + k_{\omega 2} \ \sigma_{\omega \max 2} \right)^2 + 3 \left(k_{t2,a} \ \tau_{t \max 2} \right)^2} \qquad (4)$$

$$\sigma_{v2,e} = \sqrt{\left(\sigma_{b \max 2} + k_{ax2,e} \ \sigma_{ax2} \right)^2 + \left(k_{s2,e} \ \sigma_{s2} + k_{\omega 2} \ \sigma_{\omega \max 2} \right)^2 + 3 \left(k_{t2,e} \ \tau_{t \max 2} \right)^2} \qquad (5)$$

The correction factors k_{ax2} describing the influence the axial force has on the loading combination, k_{s2} describing the influence of tooth bending, shear and pressure and k_{t2} describing the influence the torsional contribution has take into consideration the introduction of flank loading in the notch area of the hub and are dependant upon the rigidity of the joint and the hub restraint.
To determine the critical stress in the notch area of the shaft the individual resultant equivalent stresses from Eqns.(4) and (5) must be compared to one another and the maximum value taken. The equivalent stress is separately calculated for static and dynamic load cases.
The calculation principles behind the calculation of load capacity are universally applicable and are valid for splined shafts with any flank profile. In order to determine them the geometry dependent parameters must be ascertained in each case (for example by means of finite element analysis), which have already been determined for involute splines with a tooth profile according to DIN 5480 and which are to be included in Part 2 of DIN 5466 (under development at the moment).

References

Decker, K.-H., "Maschinenelemente - Gestaltung und Berechnung", Carl Hanser Verlag München, 1990

Dietz, P., "Die Berechnung von Zahn- und Keilwellenverbindungen", published oneself Büttelborn, 1978

DIN 5466 E, Draft of „Tragfähigkeitsberechnung von Zahn- und Keilwellen-Verbindungen", DIN Normausschuß Antriebstechnik Frankfurt 1996

DIN 5480, "Zahnwellen-Verbindungen mitt Evolventenflanken", Teil 1 bis 16, Beuth Verlag Berlin, 1991

Kohl, G., "Ein Ansatz zur Berechnung der Zahnfußspannungen an Zahnwellenverbindungen", PhD Thesis TU Clausthal, 1986

Schäfer, G., "Der Einfluß von Oberflächenbehandlungen auf das Verschleißverhalten flankenzentrierter Zahnwellen-Verbindungen mit Schiebesitz", PhD Thesis TU Clausthal, 1995

Schöpf, H.J., "Festigkeitsuntersuchungen an Zahnwellen-Verbindungen mit Spannungsoptik und Dauerschwingversuchen, PhD Thesis TU München, 1976

Villmer, F.J., "Zum Mechanismus der Lastverteilung in Zahnwellen-Verbindungen", PhD Thesis TU Clausthal, 1984

Wesolowski, K., "Dreidimensionale Beanspruchungszustände und Festigkeitsnachweis drehmomentbelasteter Zahnwellen-Verbindungen unter elastischer und teilplastischer Verformung", PhD Thesis TU Clausthal, 1996

Zapf, R., "Betriebs- und Verschleißverhalten flankenzentrierter Zahnwellenverbindungen mit Schiebesitz", PhD Thesis TU Clausthal 1986

Dipl.-Ing. Uwe Burgtorf
Technische Universität Clausthal
Fritz-Süchting-Institut für Maschinenwesen
Robert-Koch-Straße 32, 38678 Clausthal-Zellerfeld, Germany
Tel: +49 5323 722270, Fax: +49 5323 723501, E-Mail: burgtorf@imw.tu-clausthal.de